Layered Crystalline Barium Phosphate Organofunctionalized for Cation Removal

Angélica M. Lazarin and Claudio Airoldi*

Instituto de Química, Universidade Estadual de Campinas, Caixa Postal 6154, 13084-971 Campinas, SP, Brazil

Received August 26, 2005. Revised Manuscript Received December 13, 2005

The available hydroxide groups inside the lamellar cavity of barium phosphate (BaP) were reacted with the silyating agents $(RO)_3Si(CH_2)_3L_x$ ($L_1 = NH_2$, $L_2 = NH(CH_2)_2NH_2$, and $L_3 = NH(CH_2)_2NH(CH_2)_2NH_2$), to yield organofunctionalized nanomaterials $BaPSiL_1$, $BaPSiL_2$, and $BaPSiL_3$. The amount of organofunctional groups covalently attached to the inorganic layer was 1.24, 1.46, and 1.23 mmol g^{-1}, respectively. The basic nitrogen center atoms attached to the pendant organic chains adsorb $FeCl_3$, $CuCl_2$, and $ZnCl_2$ from ethanol solutions to give well-established isotherms at 298 ± 1 K. The results obtained in flow experiments showed a retention and recovery of ca. 100% of the metal ion with packed $BaPSiL_x$ columns from solution containing a mixture of these cations. The energetic effect caused by iron, copper, and zinc ion interactions was determined through calorimetric titration at the solid−liquid interface and gave a net thermal effect that enabled the calculation of the exothermic enthalpic values and the equilibrium constants. The complete thermodynamic data showed that the system has favorable enthalpic, Gibbs free energy, and entropic values. The cation removal properties were used with packed columns to successfully determine these cations in ethanol used as fuel sources.

Introduction

The self-organized molecular assembly producing a desired organic species on an inorganic solid surface is a methodology applied to synthesize inorganic−organic hybrids.[1] A material designed using mild experimental reaction conditions through soft-chemical routes is, instead of other procedures, a promising strategy since the resulting layered inorganic−organic hybrid may have, in a unique nanostructure, properties strongly controlled by host−guest interactions. A wide variety of such classes of hybrids have been prepared by intercalation reactions and their properties have been investigated.[2] Among well-established intercalation reactions, lamellar compounds can potentially use the available silanol groups disposed in the interlamellar layer to immobilize organic units, by exploring the versatile attributes of silyating agents.[3] From this process, the final material may have merit in practical applications due to the thermal and chemical stabilities of the hybrid. The silylation layer aggregates the chosen component to the original nanomaterial, enabling organic functional attachments to produce novel hybrids, by adding activities such as film-forming abilities[4] and adsorptive properties.[5]

The silylating reaction is characterized by the displacement of active hydrogen atoms originally attached to silanol groups by organosilyl derivatives of silane coupling agents having the general formula $(R'O)_3SiR$.[6,7] This organic molecule contains the moiety R in which functional centers are attached to the organic chain while the alkoxy R′O groups are normally derived from common alcohols. These latter groups are easily hydrolyzed when dispersed in water or simply by the water of hydration that exists on the substrate surface during the chemical process. The selection of a desirable functional group on the R moiety during the immobilization depends on the subject of each application.[6,8] Thus, the R groups are chosen to exploit, for instance, wettability, corrosion, resistance, interfacial electrical resistance, and adhesive functions or cation adsorption.[6,8]

The application of such immobilization methods can yield grafted surfaces, where defined coupling agents are covalently bonded onto the inorganic supports. The final products of the anchored surfaces have great utility in many areas such as chemically bonded phases in chromatography,[9] preconcentration and extraction of cations from solutions,[10] use in catalytic processes,[11] and biomaterial immobilization.[12]

Among a variety of matrixes, such as oxides, glasses, and clay minerals, which contain available OH-end groups bonded on the respective surfaces, silica gel has been

* To whom correspondence should be addressed. E-mail: airoldi@iqm.unicamp.br.

(1) Ogawa, M.; Takizawa, Y. *Chem. Mater.* **1999**, *11*, 30.
(2) Alberti, G., Bein T., Eds. *Comprehensive Supramolecular Chemistry*; Pergamon Press: New York, 1996; Vol. 7.
(3) Yde, Y.; Ogawa, M. *Chem. Commun.* **2003**, 1262.
(4) Ogawa, M.; Miyoshi, M.; Kuroda, K. *Chem. Mater.* **1998**, *10*, 3787.
(5) Ogawa, M.; Okutomo, S.; Kuroda, K. *J. Am. Chem. Soc.* **1998**, *120*, 7361.
(6) Jal, P. K.; Patel, S.; Muhra, B. K. *Talanta* **2004**, *62*, 1005.
(7) Sales, J. A. A.; Airoldi, C. *Thermochim. Acta* **2005**, *427*, 77.
(8) Arakaki, L. N. H.; Airoldi, C. *Quim. Nova* **1999**, *22*, 246.
(9) Silva, C. R.; Airoldi, C.; Collins, K. E.; Collins, C. H. *J. Chromatogr. A* **2004**, *22*, 632.
(10) Prado, A. G. S.; Airoldi, C. *Anal. Chim. Acta* **2001**, *432*, 201.
(11) Moura, J. A.; Araujo, A. S. A.; Coutinho, C. S. L. S.; Aquino, J. M. F. B.; Silva, A. O. S.; Souza, M. J. B. *J. Therm. Anal. Calorim.* **2005**, *79*, 435.
(12) Airoldi, C.; Monteiro, A. O. C., Jr. *J. Appl. Polym. Sci.* **2000**, *77*, 797.

10.1021/cm0519333 CCC: $33.50
Published on Web 03/29/2006

extensively modified with a great variety of alkoxysilane agents containing a variety of functionalities, for example, amino,[13] mercaptan,[14] epoxy,[7,15] and methacrylate.[16]

Nowadays, increasing interest in inorganic materials has been focused not only on those obtained from natural sources but also on properties associated with surface reactivity. One of these inorganic nanomatrixes are divalent metal phosphates that are normally synthesized as water-insoluble layered crystalline compounds of the general formula $M(H_2PO_4)_2$ (M = Mg, Ca, Sr, Ba, etc.). This class of compounds presents as their main characteristics a well-organized lamellar structure that allows them to act as excellent matrixes for intercalation reactions,[17−20] However, immobilization reactions have not yet been explored.

The present investigation reports the synthesis of a layered barium phosphate and its further reaction with silylating agents with increasing organic chains containing nitrogen basic atoms, $(RO)_3Si(CH_2)_3L_x$ (R = CH_3 or C_2H_5 and L_1 = NH_2, L_2 = $NH(CH_2)_2NH_2$, and L_3 = $NH(CH_2)_2NH(CH_2)_2NH_2$). The new nanomaterials with pendant silylating moieties inside the nanospace cavity of the original lamellar compound were characterized and the retention capacities and the thermal effects of removing Fe(III), Cu(II), and Zn(II) cations from ethanol solutions at the solid/liquid interface were determined. The application of the new hybrids to preconcentrate cations from commercial ethanol is also reported.

Experimental Section

Materials. All chemicals were of reagent grade. Barium chloride (Merck), calcium chloride (Fisher), dibasic ammonium phosphate (Synth), ethanol (Synth), and Cu(II) (Vetec), Zn(II) (Vetec), and Fe(III) (Aldrich) chlorides were used for all preparations. The silylating agents (Aldrich) of the general formula $(RO)_3Si(CH_2)_3L_x$ (L_1 = NH_2, L_2 = $NH(CH_2)_2NH_2$, and L_3 = $NH(CH_2)_2NH(CH_2)_2NH_2$ were used as-received. Commercial alcohol samples were obtained directly from three different production units plants.

Instrumentation. Barium and phosphorus elemental analyses[21,22] were determined through atomic absorption spectroscopy using a Perkin-Elmer Model 5100 atomic absorption spectrometer and through a spectrophotometric method using a Shimadzu Model MultiSpec-1501 spectrophotometer, respectively. The amount of carbon, hydrogen, and nitrogen was obtained using a Perkin-Elmer model PE 2400 instrument. The cation content in solution was determined by using a Perkin-Elmer Model 5100 atomic absorption spectrometer.

The scanning electron microscopic (SEM) images were obtained for samples dispersed on a double-faced conducting tape affixed on an aluminum support. The samples were coated with gold using a low-voltage sputtering Balzer MED 020 apparatus and the measurements were carried out on a JEOL JSM-T300 scanning electron microscope and X-ray energy dispersive spectrometer (EDS) from Northern Instruments.

The nuclear magnetic resonance spectra of the solid material were obtained on an AC 300/P Bruker spectrometer at room temperature at 121.0 and 59.6 MHz for phosphorus and silicon, respectively. A pulse repetition time of 3 s and contact time of 3 ms were used for $^{29}Si\{^1H\}$ CPMAS experiments.

Preparation. Barium phosphate (BaP) was prepared as previously reported.[17] Briefly, to a dilute solution of barium chloride dehydrate was slowly added a 1.50 mol dm^{-3} dibasic ammonium phosphate solution and the mixture was heated to 360 K. The suspension formed was stirred for 1 h, when the solid started to settle out. The solid was filtered and dried under vacuum at 320 K. Finally, the resulting compound was heated at 440 K for 48 h to eliminate ammonia.

Silylation. The same procedure was employed to synthesize the three new hybrids. Thus, 5 g of the recently prepared crystalline lamellar phosphate barium was immersed in 100 cm^3 of dry toluene with stirring. To this solution 10.0 cm^3 of silylating agent $(RO)_3Si(CH_3)L_x$ (L_1 = NH_2, L_2 = $NH(CH_2)_2NH_2$, and L_3 = $NH(CH_2)_2NH(CH_2)_2NH_2$) were added and the mixture was stirred for 8 h under an argon atmosphere. The suspension mixture was filtered, and the solid was washed with ethanol and water and dried under vacuum at 320 K.

Adsorption. The adsorption isotherms for $FeCl_3$, $CuCl_2$, and $ZnCl_2$ from ethanol solutions were performed by using the batchwise method. For each isotherm a series of samples containing 100 mg of the barium phosphate organofunctionalized with $(RO)_3Si(CH_3)L_x$ was shaken for 3 h in an orbital bath with variable concentrations of each metal halide at a constant temperature of 298 ± 1 K. The concentration of the metal ion in solution, in equilibrium with solid phase, was determined by atomic adsorption spectrometry. The amount of cations adsorbed was determined by applying the equation $n_f = (n_a - n_s)/m$, where m is the mass of the adsorbent and n_a and n_s are the initial and the equilibrium amount of the number of moles of the metal in the solution phase, respectively.

Metal Retention. A column with dimensions of 10.0 mm length and 5.0 mm internal diameter was filled with about 1 g of the material and connected on line with a peristaltic pump. To this column 20.0 cm^3 of ethanol solutions containing 5.7, 6.5, and 6.5 mg dm^{-3} for $FeCl_3$, $CuCl_2$, and $ZnCl_2$, respectively, were passed through the column with a flow rate of 0.65 cm^3 min^{-1}. The column was initially washed with pure ethanol and afterward the cations were eluted with a mixture of ethanol/0.10 mol dm^{-3} aqueous hydrochloric acid solution in a 4:1 (v/v) proportion. The eluted metals were analyzed by atomic absorption spectrometry. Three independent cation solutions were passed through the columm and then each cation was determined in triplicate.

Calorimetric Titration. The thermal effects from iron, copper, and zinc ion interacting on $BaPSiL_x$ matrixes were followed in an isothermal LKB 2277 microcalorimetric system. A sample of approximately 10 mg of the $BaPSiL_x$ was suspended in 2.0 cm^3 of ethanol and vigorously stirred at 298.15 ± 0.20 K. After calorimetric baseline stabilization, the titrant 0.1527, 0.1497, or 0.1501 mol dm^{-3} of $FeCl_3$, $CuCl_2$, or $ZnCl_2$, respectively, was individually added to the vessel by means of a microsyringe coupled to a stainless steel needle. In an individual titration, the thermal effect caused by the reaction was recorded after each addition of the titrant. After cation adsorption onto the materials, two other titrations were carried out by using the same procedure, to follow the thermal effect of dilution of the organofunctionalized layered phosphate suspended in ethanol and also dilution of the cation solution.[10,13]

(13) Fonseca, M. G.; Filho, E. C. S.; Machado, R. S. A.; Arakaki, L. N. H.; Espínola J. E. P.; Airoldi, C. *J. Solid State Chem.* **2004**, *177*, 2316.
(14) Arakaki, L. N. H.; Airoldi, C. *Polyhedron* **2000**, *19*, 367.
(15) Moussa, N.; Ghorbel, A.; Gange, P. *J. Sol−Gel Sci. Technol.* **2005**, *33*, 127.
(16) Malucelli, G.; Priola, A.; Sangermano, M.; Amerio, E.; Zini, E.; Fabbri, E. *Polymer* **2005**, *46*, 2872.
(17) Lazarin, A. M.; Airoldi, C. *Anal. Chim. Acta* **2004**, *523*, 89.
(18) Lazarin, A. M.; Airoldi, C. *Sens. Actuators B* **2005**, *107*, 446.
(19) Wypych, F.; Schreiner, W. H.; Mattoso, N.; Mosca, D. A.; Marangoni, R.; Bento, C. A. S. *J. Mater. Chem.* **2003**, *13*, 304.
(20) Sales, J. A. A.; Airoldi, C. *J. Non-Cryst. Solids* **2003**, *330*, 142.
(21) Lazarin, A. M.; Airoldi, C. *J. Chem. Thermodyn.* **2005**, *37*, 247.
(22) Lazarin, A. M.; Gushikem, Y. *J. Braz. Chem. Soc.* **2002**, *13*, 88.

Table 1. Percentages of Carbon, Hydrogen, and Nitrogen for the Functionalized Compounds and the Amount (d) of the Attached Silylating Agents in the $BaPSiL_x$ ($x = 1, 2, 3$) Matrixes

samples	C (%)	H (%)	N (%)	*d* (mmol g^{-1})
$BAPSiL_1$	7.10	1.81	2.06	1.24
$BaPSiL_2$	10.22	2.02	4.08	1.46
$BaPSiL_3$	12.71	3.12	5.17	1.23

Results and Discussion

Barium and phosphorus elemental analysis determinations for the synthesized compound gave 41.7 and 18.0%, respectively, values which are very close to the calculated required amounts 41.7 and 18.8%, for the expected formula $Ba(H_2PO_4)_2$. From these percentage values the corresponding number of moles of each elements was calculated to give a phosphorus to barium molar ratio equal to two.

The results of carbon, hydrogen, and nitrogen elemental analyses for organofunctionalized barium phosphate are listed in Table 1. Since in all cases the precursor general silylating agent $(RO)_3Si(CH_2)_3L_x$ reacts with the available OH groups on each lamella of the barium phosphate, represented here as POH, then the proposed reaction is given:

$$3POH + (RO)_3Si(CH_2)_3L \rightarrow (PO)_3Si(CH_2)_3L + 3ROH \quad (1)$$

Based on the nitrogen elemental analysis listed in Table 1, for each new compound, which increase from L_1 to L_3, as expected, the density of the organofunctionalization was calculated, considering the establishment of a covalent bond between L and the inorganic layer, showing a slight amount found for L_2 compound.

The X-ray diffraction powder patterns for the synthetic and the functionalized organosilane compounds gave sharp peaks, indicating that the crystallinity of the original solid is maintained after organofunctionalization. The intense peak at $2\theta = 12.8°$ corresponds to an interlayer distance of 697 pm for the original lamellar compound.[17] However, the expected dependence of the interlayer distance as a function of the length of the organic chain was not detected.

The increase in interlayer distance was clearly observed, but with an upper limit close to 1576 pm for all organic groups intercalated in the lamellar compound. The increased values observed for interlayer spacing in the original crystalline lamellar compound are, therefore, related to the presence of increasingly large organic chains attached to the inorganic backbone through the Si−C covalent bond formation via silylating agents. This fact suggests that organic chains were incorporated into the interlayer nanospace. Thus, the pendant organic groups lengths were calculated as 543, 939, and 1200 pm, for the organic moieties: $-(CH_2)_3NH_2$, $-(CH_2)_3NH(CH_2)_2NH_2$, and $-(CH_2)_3NH(CH_2)_2NH(CH_2)_2NH_2$ attached to the inorganic backbone.[23] Based on these data, it is expected that the organic chains are oriented in inclined and possibly alternating positions between the two successive layers into the gallery space.[13,24]

Clear evidence of the alkoxysilane reaction with the available phosphate groups of the original crystalline compound is given by the ^{29}Si MAS NMR spectra, illustrated in Figure 1 for the L_1 organofunctionalized matrix. For all spectra, peaks appeared at −58 and −67 ppm due to the presence of silicon bonded to an organic group in the different chemical environments. Thus, the second peak at −58 ppm is related to silicon bonded to an inorganic structure of the type $(PO)_2(OH)Si(L)$ or $(PO)_2(OCH_3)SiL$. Meanwhile, the signal at −66 ppm is associated with the silicon atom bonded in bulk, to represent the species $(PO)_3SiR$. The significant intensity of the signal at −66 ppm suggests than an effective organofunctionalization of the organic group occurred and the results confirm the presence of the organosilane covalently bonded to the inorganic backbone of the precursor matrix.[25]

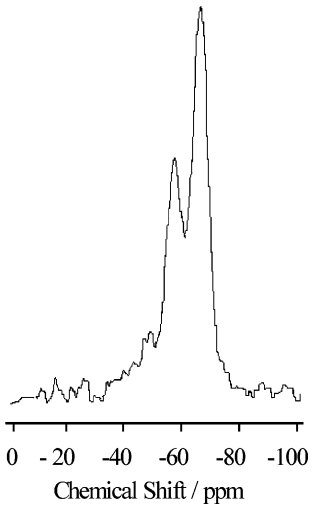

Figure 1. ^{29}Si MAS NMR spectrum of barium phosphate intercalated with L_1 molecule.

Phosphorus nuclear magnetic resonance for barium phosphate in the solid state presented a peak centered at −2.4 ppm. The main peak is accompanied by symmetrical sidebands due to the effect of chemical shift anisotropy.[25] When the original matrix is organofunctionalized, similar spectra were observed for all cases and a single ^{31}P NMR peak centered at −2.2 ppm was also observed.

The scanning electron microscopic (SEM) photographs of barium phosphate and also for the organofunctionalized compound with L_3 molecule are shown in Figure 2. The crystal morphology of these compounds is clearly lamellar for all functionalized compounds, in good agreement with the expected structural characteristics. The morphology of intercalated material is very similar to the image found for the host matrix. These results are very important in order to obtain pillared compounds with a high degree of crystallinity.[26] In the EDS image the white dots are silicon atoms and correspond to emission lines with an energy of 168 kJ. No particle agglomerates[27] can be observed with barium phosphate.

Adsorption Isotherms. Commercial ethanol in Brazil normally designates a mixture of ethanol with a low percentage of water. In use, other additives define its application in diverse fields such as in the food industry, in alcohol chemistry, or as automotive engine fuels. One positive aspect of

(23) Fonseca, M. G.; Airoldi, C. *Chem. Mater.* **2002**, *14*, 175.
(24) Ek, S.; Iiskola, E. I.; Nunisto, L. *J. Phys. Chem.* **2004**, *108*, 9650
(25) Dion, A.; Berno, B.; Hall, G.; Filiaqqi, M. J. *Biomaterials* **2005**, *26*, 4486.
(26) Carlino, S.; Hudson, M. J.; Locke, W. J. *J. Mater. Chem.* **1997**, *7*, 813.
(27) Lazarin, A. M.; Landers, R.; Kholin, Y. V.; Gushikem, Y. *J. Colloid Interface Sci.* **2002**, *254*, 31.

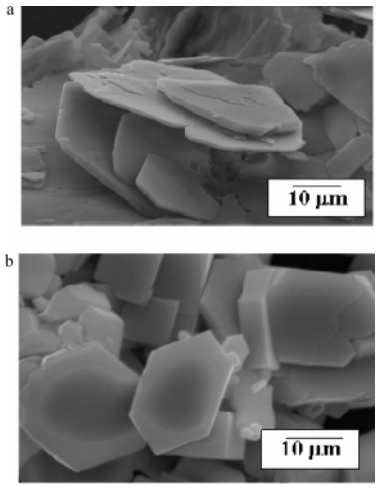

Figure 2. SEM photographs of pure barium phosphate (a) and intercalated with L_3 (b) molecule.

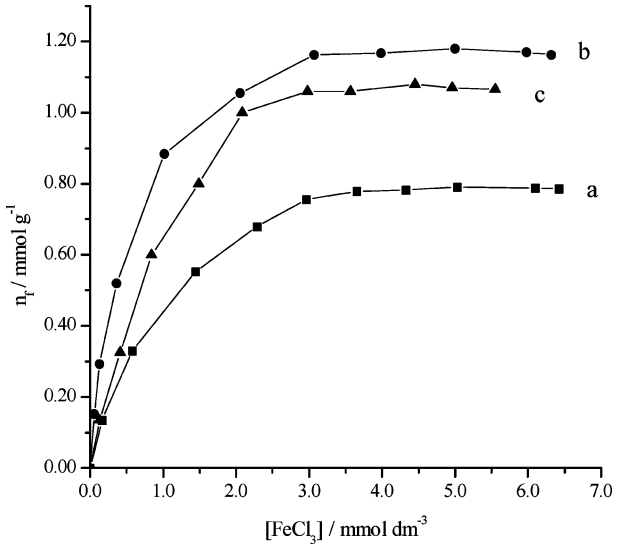

Figure 3. Adsorption isotherm for $FeCl_3$ from ethanol solution at 298 ± 1 K. (a) $BaPSiL_1$, (b) $BaSiLP_2$, and (c) $BaPSiL_3$.

ethanol research as a fuel has been the development of methods to determine traces of metals that result from the extraction operation from sugar cane. The presence of cations in ethanol fuel can induce corrosion in the vehicle components in contact with the liquid.[28] For cation determinations, the first step in the usual procedures has been evaporation of the liquid to dryness, which is obviously time-consuming.[29]

To verify the usefulness of the present nanomaterials for cation adsorption from ethanol solutions, adsorption isotherms of selected metals, Fe^{3+}, Cu^{2+}, and Zn^{2+}, were explored. Thus, the adsorption isotherms for these three metals from ethanol solutions onto organofunctionalized surface, represented by $BaPSiL_x$, are shown in Figures 3−5. The same adsorption procedure with the original lamellar compound showed that no cation was adsorbed.

The organofunctionalized species on the solid surface behaves, for all cases, as a neutral ligand and, thus, MCl_z diffuses from the solution phase into the solid surface as a neutral species. These metal cations are coordinated to the

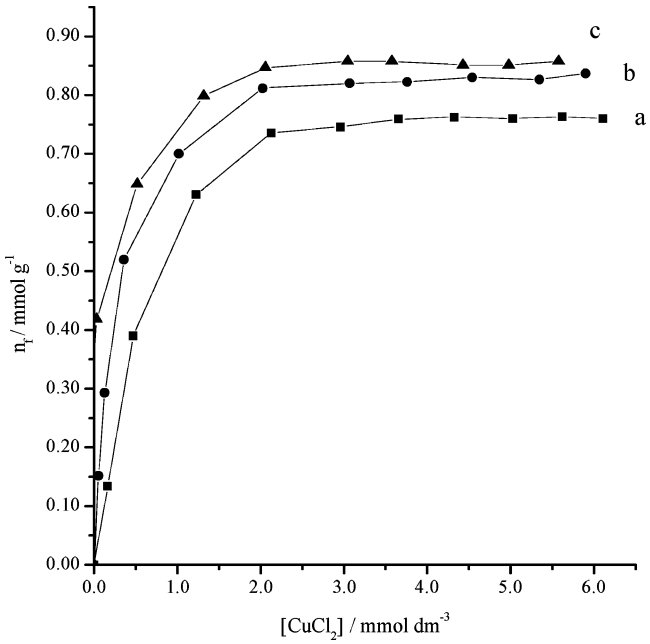

Figure 4. Adsorption isotherm for $CuCl_2$ from ethanol solution at 298 ± 1 K. (a) $BaPSiL_1$, (b) $BaPSiL_2$, and (c) $BaPSiL_3$.

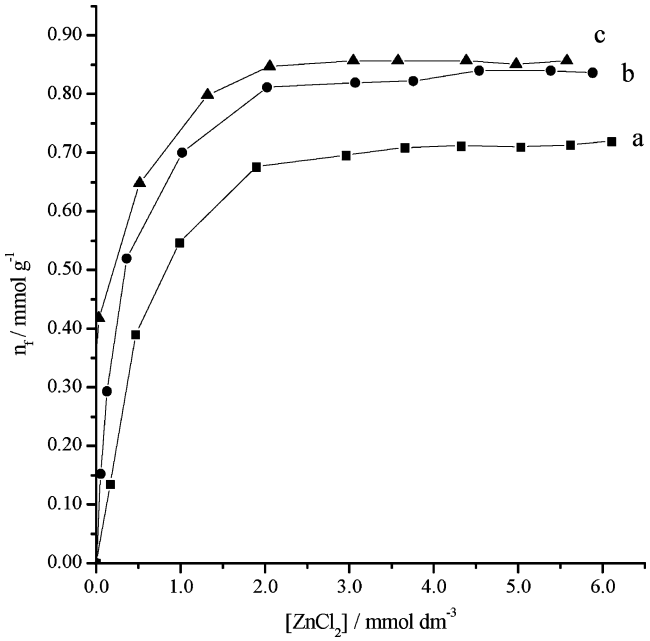

Figure 5. Adsorption isotherm for $ZnCl_2$ from ethanol solution at 298 ± 1 K. (a) $BaPSiL_1$, (b) $BaPSiL_2$, and (c) $BaPSiL_3$.

nitrogen atoms and the anions can be in the inner coordination sphere, bonded to the metal ion or remaining in the outer sphere, balancing the charge. In any case, the equilibrium of complex formation with the electrically neutral grafted ligands can formally be expressed as[30,31]

$$BaPSiL_x + MCl_z = BaPSiL_x \cdot MCl_z \qquad (2)$$

The solid adsorption capacity for the metal halide by the $BaPSiL_x$ matrixes depend on the nature of the complex formed on the surface and also on the affinity of the metal

(28) Fujiwara, S. T.; Gushikem, Y.; Alfaya, R. V. S. *Colloid Surf.* **2001**, *178*, 135.
(29) Bruning, I. M. R.; Mal, E. E B. *Bol. Tec. Petrobras* **1982**, *25*, 217.
(30) Lazarin, A. M.; Airoldi, C. *J. Inclusion Phenom.* **2005**, *51*, 33.
(31) Lazarin, A. M.; Gushikem, Y. *J. Mater. Chem.* **2000**, *10*, 2526.

Table 2. Adsorption Capacity (n_f^{max}) for $FeCl_3$, $CuCl_2$, and $ZnCl_2$ by $BaPSiL_x$ ($x = 1, 2, 3$) Matrixes

	n_f^{max} (mmol g^{-1})		
samples	$FeCl_3$	$CuCl_2$	$ZnCl_2$
$BaPSiL_1$	0.79	0.76	0.71
$BaPSiL_2$	1.18	0.83	0.85
$BaPSiL_3$	1.08	0.84	0.85

Table 3. Preconcentration and Recovery of $FeCl_3$, $CuCl_2$, and $ZnCl_2$ from Ethanol Solution by $BaPSiL_x$ ($x = 1, 2, 3$) Matrixes

	flow rate (cm^3 min^{-1})	adsorbed (μmol)	recovered (μmol)
		$BaPSiL_1$	
Fe(III)	0.65	0.98	0.97 ± 0.01
Cu(II)	0.65	0.98	0.97 ± 0.01
Zn(II)	0.62	0.93	0.92 ± 0.01
		$BaPSiL_2$	
Fe(III)	0.70	1.05	1.03 ± 0.01
Cu(II)	0.65	0.98	0.97 ± 0.01
Zn(II)	0.60	0.90	0.89 ± 0.01
		$BaPSiL_3$	
Fe(III)	0.60	0.90	0.88 ± 0.01
Cu(II)	0.65	0.98	0.97 ± 0.01
Zn(II)	0.64	0.95	0.95 ± 0.01

for the particular attached ligand.[24,32] The maximum adsorption capacity, n_f^{max}, for each metal halide through organofunctionalized barium phosphate is listed in Table 2. It is observed that n_f^{max} is highest for $FeCl_3$ for all organofunctionalized compounds and the other two adsorbents present nearly the same adsorption. Here, it was observed that the attached organic groups form complexes with all cations and show values that are slightly higher for the bidentate (L_2) and tridentate (L_3) ligands, in comparison with the monodentate (L_1) molecule.

Retention of Cations. The results obtained from the experiments carried out by passing a mixture of the three metals through the column packed with $BaPSiL_x$ matrixes are summarized in Table 3. Experiments carried out in triplicate for each material showed that, in every case, the column retained the cations and they are then released by an acidic solution with nearly 100% efficiency. Thus, the same efficiency is observed in all experiments. For example, when the column was packed with $BaPSiL_1$, three distinct determinations involving alcoholic Fe(III) solutions gave recoveries of 0.97, 0.97, and 0.96 μmol, with the medium value of 0.97 μmol. These values reflect a high efficiency for these organofunctionalized nanomaterials.

Cation Determinations from Fuel Ethanol. The adsorption method was used to determine cations present in commercial ethanol from three different production plants by passing 300 cm^3 of sample through a packed column. Complete elution of the metals adsorbed was carried out using about 40 cm^3 of ethanol/water mixture with a water mole fraction of 0.80, with in triplicate experiments. In each experiment the efficiency was close to that obtained above.

The results of the preconcentration of cations in ethanol fuels from plants A, B, and C, using $BaPSiL_x$ columns, are listed in Table 4. The data provided by plant B indicated an amount of copper of 5000 μg dm^{-3}, determined through

Table 4. Preconcentration of Cations from Fuel Ethanol from Different Sources

	concentration found (μg dm^{-3})		
plant	Fe(III)	Cu(II)	Zn(II)
		$BaPSiL_1$	
A	4 ± 1	200 ± 20	2.9 ± 0.2
B	a	5000 ± 50	4.8 ± 0.5
C	9 ± 1	9 ± 3	2.6 ± 0.3
		$BaPSiL_2$	
A	4 ± 1	201 ± 20	2.8 ± 0.1
B	a	5000 ± 50	4.7 ± 0.5
C	8 ± 1	9 ± 3	2.6 ± 0.2
		$BaPSiL_3$	
A	4 ± 1	200 ± 20	2.8 ± 0.1
B	a	5000 ± 50	4.8 ± 0.5
C	8 ± 1	8 ± 3	2.5 ± 0.3

[a] Not detected.

atomic absorption. Using this same alcohol in our laboratory, we obtained the same value after preconcentration, with the copper being determined in the eluted sample by using the same technique. For A and C plants the values provided were 200 and 9 μg dm^{-3}, which are very close to those determined in our experiments. Thus, these similar values demonstrated the accuracy of our laboratory determination. This high copper concentration in comparison with other alcohol sources can be explained by considering that this industrial operation uses a copper distillation column, while the plants A and C used stainless steel columns.

Other cation values are very low according to the supplies: 4 and 9 μg dm^{-3} for A and C plants for iron and 2.9, 4.8, and 2.6 μg dm^{-3} for A, B, and C plants for zinc. These values depend on the degree of corrosion of the distillation equipment.[31] As observed in Table 4, the results obtained are suitable for justifying the methodology used, which could be recommended for such cations found in commercial alcohol.

Calorimetry. The interactive effect of the available nitrogen basic atoms attached to the pendant chains covalently bonded to the inorganic layer, with iron, copper, and zinc cations, can be determined at the solid/liquid interface, by using a sequence of three independent calorimetric titrations: (a) thermal effect of reaction, Q_r, where the ethanolic cation solution is added to a suspension of about 10 mg of the inorganic matrix in 2.0 cm^3 of ethanol; (b) thermal effect of dilution, Q_{dil}, by adding the same ethanolic cation solution into an identical volume of ethanol; and (c) thermal effect of hydration, Q_h, that involves the addition of ethanol to a matrix in suspension. The effects of the thermodynamic cycle for this series of interactions involving $BaPSiL_x$ with metallic cations can be represented by considering ethanol (EtOH) as a calorimetric solvent(s):

$$BaPSiL_x(s) + MCl_z(s) = BaPSiL_x{\cdot}MCl_z(s), \qquad Q_r \quad (3)$$

$$MCl_z(s) + n\text{EtOH} = MCl_z{\cdot}n\text{EtOH}(s), \qquad Q_{dil} \quad (4)$$

$$BaPSiL_x(s) + n\text{EtOH} = BaPSiL_x{\cdot}n\text{EtOH}(s), \qquad Q_h \quad (5)$$

$$BaPSiL_x{\cdot}n\text{EtOH} + MCl_z{\cdot}n\text{EtOH} = BaPSiL_x{\cdot}MCl_z(s) + 2n\text{EtOH}, \qquad Q_{int} \quad (6)$$

Reactions 3−5 represent the individual calorimetric titration experiments, carried out in duplicate for each determination.

(32) Padilha, P. D.; Rocha, J. C.; Moreira, J. C.; Campos, J. T. D.; Federici, C. D. *Talanta* **1997**, *45*, 317.

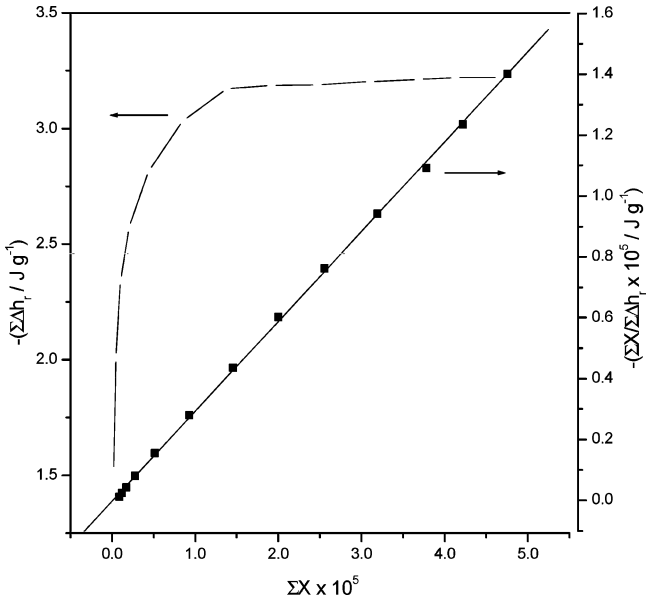

Figure 6. Isotherm for the integral enthalpy of intercalation $\sum\Delta h_r$ vs molar fraction, $\sum X$, obtained from a calorimetric titration of 0.0100 g of $BaPSiL_2$ suspended in 2.0 cm^3 of ethanol, with 0.30 mol dm^{-3} copper ion in the same solvent at 298.15 ± 0.20 K. The straight line is the linearized form of the isotherm.

The thermal effects of reaction for each experimental point of the calorimetric titration were considered for calculation of the net thermal effect (Q_{int}) of these interactions.[33,34]

From the set of thermal effects related to direct titration and dilution, recorded as joules per gram, the enthalpy of reaction ($\sum\Delta h_r$) and the enthalpy of interaction ($\sum\Delta h_{int}$) can be calculated, in joules per mole, by using the previous data adjusted to the modified Langmuir equation. Thus, a sequence of values was obtained from the calorimetric data to enable the calculation of the net enthalpy of interaction to form a monolayer per unit mass of matrixes, Δh_{int}, by using eq 7, a modified Langmuir model adapted to describe several types of systems.[33,34]

$$\sum X/\sum\Delta h_r = 1/(K-1)\Delta h_{int} + \sum X/\Delta h_{int} \qquad (7)$$

where $\sum X$ is the sum of the molar fractions of the cation remaining in solution after interaction, $\sum\Delta h_r$ is the enthalpy of cation/$BaPSiL_x$ interaction obtained by dividing the thermal effect resulting from $\sum Q_{int}$ by the number of moles of adsorbed cation, and K is a proportionality constant that includes the equilibrium constant. Therefore, a $\sum X/\sum\Delta h_r$ vs $\sum X$ plot gives Δh_{int} and K values from the angular and linear coefficients, respectively, after the linearization of the equation, as shown in Figure 6. The calculation of ΔH was based on the expression $\Delta H = \Delta h_{int}/n_s$, were n_s is the number of adsorbed moles after reaching calorimetric equilibrium. The values are listed in Table 5.

The net thermal effect obtained from the calorimetric titration technique enables the determination of the thermal effects associated with the interaction of a cation and $BaPSiL_x$, which gave the exothermic enthalpic values, listed in Table 5. For all cases, these values increased with the number of basic nitrogen atoms on the pendant organic chains, to give the order $BaPSiL_x$ (1−3), when the same cation interacts with the sequence of matrixes. This behavior is associated with different kinds of complexes formed between basic nitrogen atoms and the cations. The coordination compound formed should be more favorable for multidentate basic nitrogen atoms, as reflected in the enthalpic results in Table 5. Nonlinear behavior in enthalpy was observed on passing from mono- to tridentate moieties.[35] As observed, the enthalpic changes are exothermic, decreasing in the order Fe(III) > Cu(II) > Zn(II), this sequence being identical to that obtained for n_f values. The highest values obtained for iron reflect the best interactive effect for stable complex formation. This set of results is, to our knowledge, the first quantitative determination for an organofunctionalized lamellar phosphate. Despite the low enthalpic values obtained, the surface of these matrixes presented a large number of basic centers, reflected in the number of moles adsorbed. This property can be potentially useful for applying this material to remove cations that normally appear in ethanol used as engine fuel.[27,31,32]

The Gibbs free energy was calculated from the expression $\Delta G = -RT \ln K$ and the results are listed in Table 5. The values indicate that spontaneous processes occurred and follow the order Fe(III) < Cu(II) < Zn(II). As observed before,[36] there is a correlation between the Gibbs free energy of hydration and the correspondent energy obtained for each reaction. For example, copper presents the largest free energy change, −22.7 ± 0.1, −23.9 ± 0.1, and 22.7 ± 0.1 kJ mol^{-1} for $BaPSiL_1$, $BaPSiL_2$, and $BaPSiL_3$, respectively, with the lowest cation hydration free energy of −2016 kJ mol^{-1}. Compare this value with −1963 and −1848 kJ mol^{-1} for zinc and iron,[37] respectively. The missing thermodynamic data, the entropy values, were calculated from $\Delta G = \Delta H -$

Table 5. Thermodynamic Data for the Interaction of $BaPSiL_x$ (x = 1, 2, 3) Matrixes with $FeCl_3$, $CuCl_2$, and $ZnCl_2$ in Ethanol Solution, at 298.15 ± 0.20 K

	n^s (mmol g^{-1})	$-\Delta h_{int}$ (J g^{-1})	$-\Delta H°$ (kJ mol^{-1})	$K° \times 10^{-3}$	ln $K°$	$-\Delta G°$ (kJ mol^{-1})	$\Delta S°$ (J mol^{-1} K^{-1})
			$BaPSiL_1$				
Fe(III)	0.98	6.12	6.24 ± 0.37	8.27	9.02	22.4 ± 0.1	54 ± 1
Cu(II)	0.95	5.21	5.48 ± 0.20	9.32	9.14	22.7 ± 0.1	58 ± 1
Zn(II)	0.91	4.13	4.54 ± 0.19	11.85	9.38	23.3 ± 0.1	63 ± 1
			$BaPSiL_2$				
Fe(III)	1.25	9.11	7.30 ± 0.34	15.06	9.62	23.9 ± 0.1	56 ± 1
Cu(II)	1.11	6.91	6.23 ± 0.26	13.35	9.50	23.6 ± 0.1	58 ± 1
Zn(II)	1.08	6.50	6.02 ± 0.20	15.06	9.62	23.9 ± 0.1	60 ± 1
			$BaPSiL_3$				
Fe(III)	1.12	9.23	8.24 ± 0.21	9.32	9.14	22.7 ± 0.1	48 ± 1
Cu(II)	0.94	7.47	7.95 ± 0.19	8.27	9.02	22.4 ± 0.1	48 ± 1
Zn(II)	0.95	6.69	7.05 ± 0.22	15.06	9.62	23.9 ± 0.1	57 ± 1

$T\Delta S$ and the results are also listed in Table 5. These values suggest that, during complex formation, the desolvation disturbs the structure of the reaction medium to promote the disorganization of the system and, consequently, leads to an increase in entropy.[35,36] The highest entropic values were observed for cations with the largest hydration volumes and illustrate the principle that the loss of water of hydration leads to a disorganization of the final system.[36] For instance, zinc, with a hydration volume of 178.2 $cm^3\ mol^{-1}$, gave entropic values of 63 ± 1, 60 ± 1, and 57 ± 1 J $mol^{-1}\ K^{-1}$ for $BaPSiL_1$, $BaPSiL_2$, and $BaPSiL_3$, respectively. For copper and iron the hydration volume values are 147.8 and 215.3 $cm^3\ mol^{-1}$. In conclusion, all thermodynamic values are favorable, with exothermic enthalpy, negative Gibbs free energy, and positive entropy, and corroborate with iron, copper, and zinc/$BaPSiL_x$ interaction at the solid/liquid interface.

Conclusions

The easily synthesized lamellar crystalline barium phosphate compound can be used as a host support for organofunctionalization. The characterization process confirms the organosilane insertions into the layered structure with silicon species uniformly dispersed in the barium phosphate lamella. The $BaPSiL_x$ matrixes can be used, without any significant loss of adsorption capacity, for various adsorption and desorption operations. An additional advantage in the present case is the high degree of organofunctionalization exhibited by the material and, consequently, the large adsorption capacity. These crystalline lamellar organofunctionalized compounds efficiently adsorb iron, copper, and zinc ions from ethanolic solutions. The quantitative interactions between cation/nitrogen basic centers attached to the pendant organic chain covalently bonded to the inorganic layer were followed calorimetrically at the solid/liquid interface to give favorable sets of thermodynamic data, such as exothermic enthalpy, negative Gibbs free energy, and positive entropic values. Their great ability for cation removal was assayed on ethanol fuel sources, showing that the inorganic−organic self-organized compounds can be efficiently used in such applications.

Acknowledgment. The authors are indebted to FAPESP for financial support and a fellowship to A.M.L. and to CNPq for a fellowship to C.A.

CM0519333

(33) Monteiro, O. A. C.; Airoldi, C. *J. Colloid Interface Sci.* **2005**, *282*, 32.
(34) Ruiz, V. S. O.; Airoldi, C. *Thermochim. Acta* **2004**, *420*, 73.
(35) Fonseca, M. G.; Airoldi, C. *J. Therm. Anal. Calorim.* **2001**, *64*, 273.
(36) Fonseca, M. G.; Airoldi, C. *Thermochim. Acta* **2000**, *359*, 1.
(37) Marcus, Y. *Ion Solvation*; Wiley: London, 1985.